




# Monotone Arc Diagrams with Few Biarcs

Steven Chaplick   


Maastricht University, The Netherlands

Henry Förster   

Universität Tübingen, Germany

Michael Hoffmann   

Department of Computer Science, ETH Zürich, Switzerland

Michael Kaufmann   

Universität Tübingen, Germany

---

## Abstract

We show that every planar graph has a monotone topological 2-page book embedding where at most  $(4n - 10)/5$  (of potentially  $3n - 6$ ) edges cross the spine, and every edge crosses the spine at most once; such an edge is called a *biarc*. We can also guarantee that all edges that cross the spine cross it in the same direction (e.g., from bottom to top). For planar 3-trees we can further improve the bound to  $(3n - 9)/4$ , and for so-called Kleetopes we obtain a bound of at most  $(n - 8)/3$  edges that cross the spine. The bound for Kleetopes is tight, even if the drawing is not required to be monotone. A *Kleetope* is a plane triangulation that is derived from another plane triangulation  $T$  by inserting a new vertex  $v_f$  into each face  $f$  of  $T$  and then connecting  $v_f$  to the three vertices of  $f$ .

**2012 ACM Subject Classification** Mathematics of computing → Combinatorics; Mathematics of computing → Graph theory; Human-centered computing → Graph drawings

**Keywords and phrases** planar graph, topological book embedding, monotone drawing, linear layout

**Digital Object Identifier** 10.4230/LIPIcs.GD.2024.11

**Related Version** *Full Version:* <https://doi.org/10.48550/arXiv.2408.14299>

**Funding** *Steven Chaplick:* supported by DFG grant WO 758/11-1.

*Michael Hoffmann:* supported by the Swiss National Science Foundation within the collaborative D-A-CH project *Arrangements and Drawings* as SNSF project 200021E-171681.

**Acknowledgements** This work started at the workshop on *Graph and Network Visualization* (GNV 2017) in Heiligkreuztal, Germany. Preliminary results were presented at the 36th European Workshop on Computational Geometry (EuroCG 2020). We thank Stefan Felsner and Stephen Kobourov for useful discussions.

## 1 Introduction

*Arc diagrams* (Figure 1) are drawings of graphs that represent vertices as points on a horizontal line, called *spine*, and edges as *arcs*, consisting of a sequence of halfcircles centered on the spine. A *proper arc* consists of one halfcircle. In *proper arc diagrams* all arcs are proper (see Figure 1a). In *plane arc diagrams* no two edges cross. Note that proper plane arc diagrams are also known as *2-page book embeddings*. Bernhard and Kainen [1] characterized the graphs that admit proper plane arc diagrams: subhamiltonian planar graphs, i.e., subgraphs of planar graphs with a Hamiltonian cycle. In particular, non-Hamiltonian maximal planar graphs do not admit proper plane arc diagrams.

To represent all planar graphs as a plane arc diagram, it suffices to allow each edge to cross the spine once [12, 13]. The resulting arcs composed of two halfcircles are called *biarcs* (see Figure 1b). Additionally, all edges can be drawn as *monotone* curves w.r.t. the spine [7, 10]; such a drawing is called a *monotone topological (2-page) book embedding* (see



© Steven Chaplick, Henry Förster, Michael Hoffmann, and Michael Kaufmann; licensed under Creative Commons License CC-BY 4.0

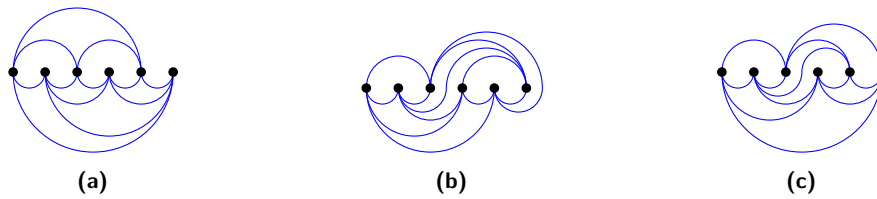
32nd International Symposium on Graph Drawing and Network Visualization (GD 2024).

Editors: Stefan Felsner and Karsten Klein; Article No. 11; pp. 11:1–11:16

Leibniz International Proceedings in Informatics



LIPICs Schloss Dagstuhl – Leibniz-Zentrum für Informatik, Dagstuhl Publishing, Germany



■ **Figure 1** Arc diagrams of the octahedron: (a) proper, (b) general, and (c) monotone.

Figure 1c). A monotone biarc is either *up-down* or *down-up*, depending on whether the left halfcircle is drawn above or below the spine, respectively. Note that a *monotone topological book embedding* is not necessarily a book embedding, even though the terminology suggests it.

In general, biarcs are needed, but *many* edges can be drawn as proper arcs. Cardinal, Hoffmann, Kusters, Tóth, and Wettstein [2, 3] gave bounds on the required number of biarcs by showing that every planar graph on  $n \geq 3$  vertices admits a plane arc diagram with at most  $\lfloor (n-3)/2 \rfloor$  biarcs and how this quantity is related to the diameter of the so-called combinatorial flip graph of triangulations. However, they allow general, not necessarily monotone biarcs. When requiring biarcs to be monotone, Di Giacomo, Didimo, Liotta, and Wismath [7, 10] gave an algorithm to construct a monotone plane arc diagram that may create close to  $2n$  biarcs for an  $n$ -vertex planar graph. Cardinal, Hoffmann, Kusters, Tóth, and Wettstein [2, 3] improved this bound to at most  $n-4$  biarcs.

As a main result, we improve the upper bound on the number of monotone biarcs.

► **Theorem 1.** *Every  $n$ -vertex planar graph admits a plane arc diagram with at most  $\lfloor \frac{4}{5}n \rfloor - 2$  biarcs that are all down-up monotone.*

It is an intriguing open question if there is a *monotonicity penalty*, that is, is there a graph  $G$  and a plane arc diagram of  $G$  with  $k$  biarcs such that every monotone plane arc diagram of  $G$  has strictly more than  $k$  biarcs? No such graph is known, even if for the stronger condition that all biarcs are monotone of the same type, such as down-up.

For general plane arc diagrams, in some cases  $\lfloor (n-8)/3 \rfloor$  biarcs are required [2, 3]. The (only) graphs for which this lower bound is known to be tight belong to the class of Kleetopes. A *Kleetope* is a plane triangulation<sup>1</sup> that is derived from another plane triangulation  $T$  by inserting a new vertex  $v_f$  into each face  $f$  of  $T$  and then connecting  $v_f$  to the three vertices of  $f$ . One might think that Kleetopes are good candidates to exhibit a monotonicity penalty. However, we show that this is not the case, but instead the known lower bound is tight.

► **Theorem 2.** *Every Kleetope on  $n$  vertices admits a monotone plane arc diagram with at most  $\lfloor (n-8)/3 \rfloor$  biarcs, where every biarc is down-up.*

So, to discover a monotonicity penalty we have to look beyond Kleetopes. We investigate another class of planar graphs: planar 3-trees. A *planar 3-tree* is built by starting from a (combinatorial) triangle. At each step we insert a new vertex  $v$  into a (triangular) face  $f$  of the graph built so far, and connect  $v$  to the three vertices of  $f$ . As a third result we give an improved upper bound on the number of monotone biarcs needed for planar 3-trees.

► **Theorem 3.** *Every planar 3-tree admits a plane arc diagram with at most  $\lfloor \frac{3}{4}(n-3) \rfloor$  biarcs that are all down-up monotone.*

<sup>1</sup> A *plane triangulation* is a triangulation associated with a combinatorial embedding. For the scope of this paper, we also consider the outer face to be fixed.

**Related work.** Giordano, Liotta, Mchedlidze, Symvonis, and Whitesides [11] showed that every upward planar graph admits an *upward topological book embedding* in which all edges are either proper arcs or biarcs. These embeddings are also monotone arc diagrams that respect the orientations of the edges and use at most one spine crossing per edge. One of their directions for future work is to minimize the number of spine crossings. We believe that our approach for undirected graphs may provide some insights. Everett, Lazard, Liotta, and Wismath [8, 9] used monotone arc diagrams to construct small universal point sets for 1-bend drawings of planar graphs, heavily using the property that all biarcs have the same *shape* (e.g., all are down-up biarcs). This result has been extended by Löffler and Tóth [14] by restricting the set of possible bend positions. They use the existence of monotone arc diagrams with at most  $n - 4$  biarcs to build universal point sets of size  $6n - 10$  (vertices and bend points) for 1-bend drawings of planar graphs on  $n$  vertices. Using Theorem 1, we can decrease the number of points by about  $n/5$ .

**Outline.** We sketch the proof of Theorem 1 in Sections 2–4, then in Section 5 the proof of Theorem 2, and finally, in Section 6 the proof of Theorem 3. Due to space constraints, some proofs are provided in the full version only.

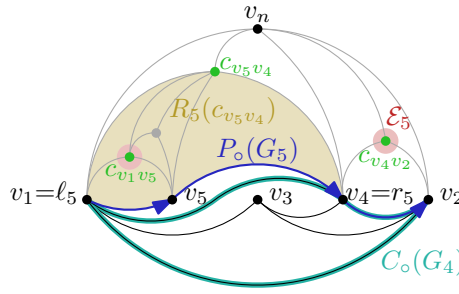
## 2 Overview of our Algorithm

To prove Theorem 1 we describe an algorithm to incrementally construct an arc diagram for a given planar graph  $G = (V, E)$  on  $n \geq 4$  vertices. Without loss of generality we assume that  $G$  is a combinatorial *triangulation*, that is, a maximal planar graph. Further, we consider  $G$  to be embedded, that is,  $G$  is a *plane* graph. As every triangulation on  $n \geq 4$  vertices is 3-connected, by Whitney’s Theorem selecting one facial triangle as the *outer face* embeds it into the plane. This choice also determines a unique outer face for every biconnected subgraph. For a biconnected plane graph  $G$  denote the outer face (an open subset of  $\mathbb{R}^2$ ) by  $F_o(G)$  and denote by  $C_o(G)$  the cycle that bounds  $F_o(G)$ . A plane graph is *internally triangulated* if it is biconnected and every inner face is a triangle. A central tool for our algorithm is the notion of a canonical ordering [5, 6]. Consider an internally triangulated plane graph  $G$  on the vertices  $v_1, \dots, v_n$ , and let  $V_k = \{v_j : 1 \leq j \leq k\}$ . The sequence  $v_1, \dots, v_n$  forms a *canonical ordering* for  $G$  if the following conditions hold for every  $i \in \{3, \dots, n\}$ :

- (C1) the induced subgraph  $G_i = G[V_i]$  is internally triangulated;
- (C2) the edge  $v_1v_2$  is an edge of  $C_o(G_i)$ ; and
- (C3) for all  $j$  with  $i < j \leq n$ , we have  $v_j \in F_o(G_i)$ .

Every internally triangulated plane graph admits a canonical ordering, for any starting pair  $v_1, v_2$  where  $v_1v_2$  is an edge of  $C_o(G)$  [5, 6]. Moreover, such an ordering can be computed by iteratively selecting  $v_i$ , for  $i = n, \dots, 3$ , to be a vertex of  $C_o(G_i) \setminus \{v_1, v_2\}$  that is not incident to a chord of  $C_o(G_i)$ . This computation can be done in  $O(n)$  time [4]. In general, a triangulation may admit many canonical orderings. We will use this freedom to adapt the canonical ordering we work with to our needs. To this end, we compute a canonical ordering for  $G$  incrementally, starting with  $v_1, v_2, v_3$ , where  $v_1v_2$  is an arbitrary edge of  $C_o(G)$ , and  $v_3$  is the unique vertex of  $G$  such that  $v_1v_2v_3$  bounds a triangular face of  $G$  and  $v_3$  is not a vertex of  $C_o(G)$ . A canonical ordering  $v_1, \dots, v_i$  for  $G_i$ , where  $3 \leq i \leq n$ , is *extensible* if there exists a sequence  $v_{i+1}, \dots, v_n$  such that  $v_1, \dots, v_n$  is a canonical ordering for  $G$ .

► **Lemma 4.** *A canonical ordering  $v_1, \dots, v_i$  for  $G_i$  is extensible  $\iff V \setminus V_i \subset F_o(G_i)$ .*



■ **Figure 2** Overview of notation used throughout the paper.

We set up some terminology used throughout the paper; refer also to Figure 2. Consider an extensible canonical ordering  $v_1, \dots, v_i$  for  $G_i$  and some vertex  $v \in V \setminus V_i$ . Let  $P_o(G_i)$  denote the path  $C_o(G_i) - v_1 v_2$  and direct it from  $v_1$  to  $v_2$ . As  $G_i$  is an induced subgraph of the plane graph  $G$  and  $v \in F_o(G_i)$  (by extensibility), all neighbors of  $v$  in  $G_i$  are on  $P_o(G_i)$ . We associate a planar region  $R_i(v)$  to  $v$  as follows. If  $d_i(v) = \deg_{G_i}(v) \leq 1$ , then  $R_i(v) = F_o(G_i)$ ; else, let  $R_i(v)$  be the open bounded region bounded by the simple closed curve formed by the part of  $P_o(G_i)$  between  $\ell$  and  $r$  together with the edges  $\ell v$  and  $r v$  of  $G$ , where  $\ell$  and  $r$  are the first and last, respectively, neighbor (in  $G$ ) of  $v$  on  $P_o(G_i)$ . We partially order the vertices in  $V \setminus V_i$  by defining  $v < v'$  if  $R_i(v) \subseteq R_i(v')$ .

A vertex  $v \in V \setminus V_i$  is *eligible* (for  $G_i$ ) if setting  $v_{i+1} = v$  yields an extensible canonical ordering  $v_1, \dots, v_{i+1}$  for  $G_{i+1}$ . Denote the set of vertices eligible for  $G_i$  by  $\mathcal{E}_i$ . Let  $e = uv$  be an arbitrary edge of  $P_o(G_i)$ , for  $i < n$ . As  $G$  is a triangulation, there exists a unique vertex  $c_e \in V \setminus V_i$  such that  $uwc_e$  bounds a triangular face of  $G$ ; we say that  $c_e$  *covers*  $e$ . Given a canonical ordering  $v_1, \dots, v_n$ , vertex  $v_i$  covers exactly the edges of  $P_o(G_{i-1})$  that are not on  $P_o(G_i)$ . Similarly, we say that  $v_i$  covers a vertex  $v$  of  $P_o(G_{i-1})$  if  $v$  is not part of  $P_o(G_i)$ . The following observations are direct consequences of these definitions and Lemma 4.

► **Corollary 5.** *A vertex  $v \in V \setminus V_i$  is eligible  $\iff R_i(v) \cap V = \emptyset \iff R_i(v) \cap \mathcal{E}_i = \emptyset$ .*

While computing a canonical ordering  $v_1, \dots, v_n$ , we also maintain an arc diagram, for short, *diagram* of  $G_i$ . This diagram must satisfy certain properties to be considered valid, as detailed below. In some cases we apply induction to handle a whole induced subgraph of  $G$ , for instance, within a (separating) triangle, at once. As a result, in certain steps, subgraph  $G_i$  may not correspond to a valid arc diagram.

Every vertex  $v_i$  arrives with  $1 - \chi$  credits, for some constant  $\chi \geq 0$ .<sup>2</sup> For these credits we can either create biarcs (at a cost of one credit per biarc), or we place them on edges of the outer face of the diagram for later use. The *costs*  $\text{cost}(D)$  of a diagram  $D$  is the sum of credits on its edges. An edge in the diagram can be one of three different types: *mountain* (proper arc above the spine), *pocket* (proper arc below the spine), or *down-up biarc*. So the diagram is determined by (1) the spine order (left-to-right) of the vertices and crossings along with (2) for every edge, its type and number of credits. The *lower envelope* of a diagram consists of all vertices and edges that are vertically visible from below, that is, there is no other vertex or edge of the diagram vertically below it. Analogously, the *upper envelope* consists of all vertices and edges that are vertically visible from above.

<sup>2</sup> For Theorem 1 we will set  $\chi = 1/5$ . But we think it is instructive to keep  $\chi$  as a general constant in our argumentation. For instance, this way it is easier to see in which cases our analysis is tight.

A diagram for  $v_1, \dots, v_i$  and  $i \in \{3, \dots, n\}$ , is *valid* if it satisfies the following invariants:

- (X1) Every edge is either a proper arc or a down-up biarc. Every edge on the upper envelope is a proper arc.
- (X2) Every mountain whose left endpoint is on  $C_o(G_i) \setminus \{v_2\}$  carries one credit.
- (X3) Every biarc carries (that is, is paid for with) one credit.
- (X4) Every pocket on  $P_o(G_i)$  carries  $\chi$  credits<sup>3</sup>.

Moreover, a valid drawing is *extensible* if it also satisfies

- (X5) Vertex  $v_1$  is the leftmost and  $v_2$  is the rightmost vertex on the spine. Edge  $v_1v_2$  forms the lower envelope of  $C_o(G_i)$ . The edges of  $P_o(G_i)$  form the upper envelope.

To prove Theorem 1 it suffices to prove the following.

► **Lemma 6.** *Let  $G$  be a maximal plane graph on  $n \geq 3$  vertices, let  $v_1, \dots, v_i$  be an extensible canonical ordering for  $G_i$ , for some  $3 \leq i < n$ , and let  $D$  be an extensible arc diagram for  $G_i$ . Then, for any  $\chi \leq \frac{1}{5}$ ,  $D$  can be extended to an extensible arc diagram  $D'$  for  $G$  with  $\text{cost}(D') \leq \text{cost}(D) + (n-i)(1-\chi) + \xi$ , for some  $\xi \leq 2\chi$ .*

**Proof of Theorem 1 assuming Lemma 6.** We may assume  $n \geq 4$ , as the statement is trivial for  $n \leq 3$ . Let  $C_o(G) = v_1v_2v_n$ , and let  $v_3$  be the other (than  $v_n$ ) vertex that forms a triangle with  $v_1v_2$  in  $G$ . Then  $v_1, v_2, v_3$  is an extensible canonical ordering for  $G_3$  in  $G$ . To obtain an extensible diagram  $D$  for  $G_3$ , place  $v_1v_3v_2$  on the spine in this order from left to right. All three edges are drawn as pockets so that  $v_1v_2$  is below  $v_1v_3$  and  $v_3v_2$ . On the latter two edges we put  $\chi$  credits each. It is easily verified that  $D$  is extensible and  $\text{cost}(D) = 2\chi$ . By Lemma 6 we obtain an extensible diagram  $D'$  for  $G$  with  $\text{cost}(D') \leq 2\chi + (n-3)(1-\chi) + 2\chi = n(1-\chi) + 7\chi - 3$ . Setting  $\chi = 1/5$  yields  $\text{cost}(D') \leq \frac{4}{5}n - \frac{8}{5}$ . As  $v_n$  is incident to a mountain on the outer face by (X5) which carries a credit by (X2),  $\text{cost}(D') - 1$  is an upper bound for the number of biarcs in  $D'$  and the theorem follows. ◀

We can avoid the additive term  $\xi$  in Lemma 6 by dropping (X5) for  $D'$ :

► **Lemma 7.** *Let  $G$  be a maximal plane graph on  $n \geq 4$  vertices, let  $v_1, \dots, v_i$  be an extensible canonical ordering for  $G_i$ , for  $3 \leq i < n$ , and let  $D$  be an extensible arc diagram for  $G_i$ . Then, for any  $\chi \leq \frac{1}{5}$ ,  $D$  can be extended to a valid arc diagram  $D'$  for  $G$  such that (1)  $\text{cost}(D') \leq \text{cost}(D) + (n-i)(1-\chi)$ , (2) Vertex  $v_1$  is the leftmost and  $v_n$  is the rightmost vertex on the spine. The mountain  $v_1v_n$  forms the upper envelope, and the pocket  $v_1v_2$  along with edge  $v_2v_n$  forms the lower envelope of  $D'$ , and (3)  $v_2v_n$  is not a pocket.*

### 3 Default vertex insertion

We prove both Lemma 6 and Lemma 7 together by induction on  $n$ . For Lemma 6, the base case  $n = 3$  is trivial, with  $D' = D$ . For Lemma 7, the base case is  $n = 4$  and  $i = 3$ . We place  $v_4$  as required, to the right of  $v_2$ , and draw all edges incident to  $v_4$  as mountains. To establish (X2) it suffices to put one credit on  $v_1v_4$  because  $v_3$  is covered by  $v_4$  and mountains with left endpoint  $v_2$  are excluded in (X2). The edge of  $D$  with left endpoint  $v_3$  is covered by  $v_4$ ; thus, we can take the at least  $\chi$  credits on it. The invariants (X1), (X3), and (X4) are easily checked to hold, as well as the statements in Lemma 7.

<sup>3</sup> As in the Greek word for pocket money:  $\chi\alpha\rho\tau\zeta\upsilon\lambda\acute{\iota}\alpha\iota$ .

11:6 Monotone Arc Diagrams with Few Biarcs

In order to describe a generic step of our algorithm, assume that we already have an extensible arc diagram for  $G_{i-1}$ , for  $i = 4, \dots, n$ . We have to select an eligible vertex  $V_i \in V \setminus V_{i-1}$  and add it using at most  $1 - \chi$  credits obtaining an extensible diagram for  $G_i$ . In this section we discuss some cases where a suitable vertex exists that can easily be added to the arc diagram, using what we call a *default insertion*. Let  $v_i$  be any vertex in  $\mathcal{E}_{i-1}$ .

We call the sequence of (at least one) edges of  $P_o(G_{i-1})$  between the leftmost neighbor  $\ell_i$  of  $v_i$  and the rightmost neighbor  $r_i$  of  $v_i$  the *profile*  $\text{pr}(v_i)$  of  $v_i$ . By (X1) each edge on the profile is a pocket or a mountain, i.e., writing  $\smile$  and  $\frown$  for pocket and mountain, respectively, each profile can be described by a string over  $\{\smile, \frown\}$ . For a set  $A$  of characters, let  $A^*$ ,  $A^k$  and  $A^+$  denote the set of all strings, all strings of length exactly  $k$  and all strings of length at least one, respectively, formed by characters from  $A$ . Let  $d_i$  denote the degree of  $v_i$  in  $G_i$ .

► **Lemma 8.** *If  $\text{pr}(v_i) \in \{\smile, \frown\}^* \smile \smile^*$ , then we can insert  $v_i$  and use  $\leq 1$  credit to obtain an extensible arc diagram for  $G_i$ . At most  $1 - \chi$  credits suffice, unless  $\text{pr}(v_i) = \smile \smile$ .*

**Proof Sketch.** We place  $v_i$  into the rightmost pocket  $p_\ell p_r$  it covers, draw  $p_\ell v_i$  and  $v_i p_r$  as pockets and all other new edges as mountains; see Figure 3. We take the  $\chi$  credits from  $p_\ell p_r$ . If  $d_i = 2$ , then we place  $\chi$  credits on each of the two pockets incident to  $v_i$  so as to establish (X4), for a cost of  $\chi \leq 1 - \chi$ , assuming  $\chi \leq 1/2$ .

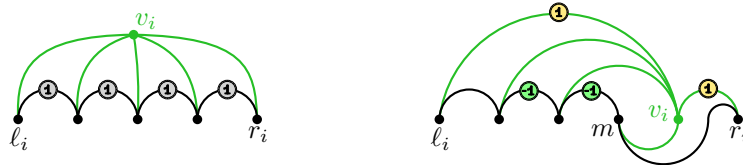


■ **Figure 3** Inserting a vertex  $v_i$  into a pocket, using  $1 - \chi$  credits (Lemma 8).

For  $d_i \geq 3$  each new mountain  $m$  from  $v_i$  to the right covers a mountain  $m'$  of  $P_o(G_{i-1})$  whose left endpoint is covered by  $v_i$ . Thus, we can take the credit from  $m'$  and place it on  $m$ . Among all mountains from  $v_i$  to the left, a credit is needed for the leftmost one only. If there is such a mountain, then we do not need the  $\chi$  credits on  $p_\ell v_i$ . And if  $v_i$  covers two or more edges to the left of  $p_\ell$ , we gain at least  $\chi$  credits from the rightmost such edge. ◀

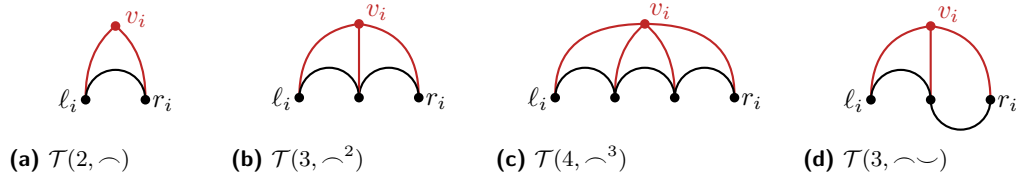
It is more difficult to insert  $v_i$  if it covers mountains only, at least if  $d_i$  is small. But if the degree of  $v_i$  is large, then we can actually gain credits by inserting  $v_i$  (see Figure 4).

► **Lemma 9.** *If  $\text{pr}(v_i) \in \frown^+$  and  $d_i \geq 5$ , then we can insert  $v_i$  and gain at least  $d_i - 5$  credits to obtain an extensible arc diagram for  $G_i$ .*



■ **Figure 4** Inserting a vertex  $v_i$  into mountains, using  $5 - d_i$  credits (Lemma 9).

An eligible vertex is *problematic* if it is of one of the four specific types depicted in Figure 5. Using Lemmas 8 and 9 we insert vertices using at most  $1 - \chi$  credits per vertex, unless all eligible vertices are problematic. This specific situation is discussed in the next section.



■ **Figure 5** The four types of problematic vertices where default insertion fails.

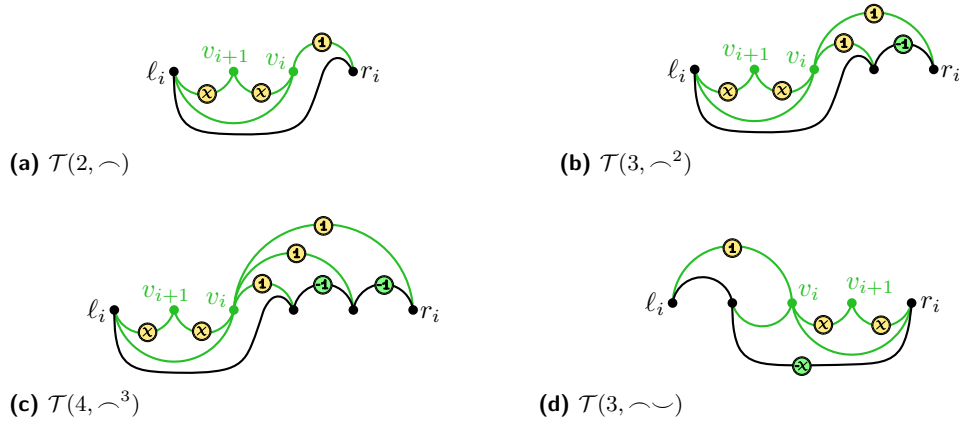
#### 4 When default insertion fails

In this section we discuss how to handle the case where all eligible vertices are problematic, that is, they cannot be handled by our default insertion. Let  $v$  be an arbitrary vertex in  $\mathcal{E}_{i-1}$ , and let  $\ell$  and  $r$  denote the leftmost and rightmost neighbor of  $v$  on  $P_o(G_{i-1})$ , respectively.

A special case arises if  $v = v_n$  is the last vertex of the canonical ordering. This case is easy to resolve, see Appendix C in the full version for details. Otherwise, we have  $i < n$  and pick a *pivot vertex*  $p(v)$  as follows: If  $v$  is  $\mathcal{T}(3, -\sphericalcap)$  we set  $p(v) = r$  and say that  $v$  has *right pivot type*, in the three remaining cases we set  $p(v) = \ell$  and say that  $v$  has *left pivot type*. Let  $pc(v) \in V \setminus V_i$  denote the unique vertex that covers the *pivot edge*  $vp(v)$ .

► **Lemma 10.** *Assume there is a vertex  $v \in \mathcal{E}_{i-1}$  such that  $pc(v)$  has only one neighbor on  $P_o(G_{i-1})$ . Then we can set  $v_i = v$  and  $v_{i+1} = p(v)$  and spend at most  $1 + 2\chi$  credits to obtain an extensible arc diagram for  $G_{i+1}$ .*

**Proof.** The resulting diagram is shown in Figure 6. The costs to establish are  $1 + \chi$  for  $\mathcal{T}(3, -\sphericalcap)$  and  $1 + 2\chi$  for the other types. Note that  $1 + 2\chi \leq 2(1 - \chi)$ , for  $\chi \leq 1/4$ . ◀

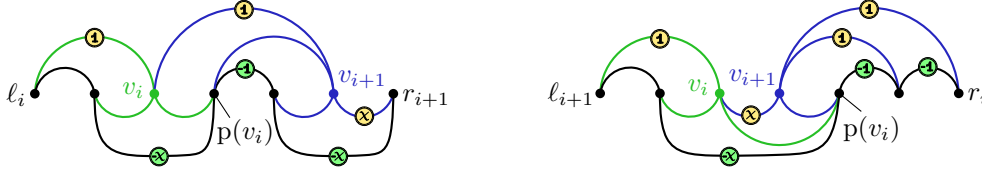


■ **Figure 6** Insertion of  $v_i$  and  $v_{i+1}$  if  $v_{i+1} = pc(v_i)$  has degree two in  $G_{i+1}$ .

► **Lemma 11.** *Assume that there are  $v, v' \in \mathcal{E}_{i-1}$  such that  $pc(v) = v'$  and at least one of  $v, v'$  has right pivot type. Then we can set  $v_i = v$  and  $v_{i+1} = v'$  and spend at most one credit to obtain an extensible arc diagram for  $G_{i+1}$ .*

**Proof.** If both  $v$  and  $v'$  have right pivot type, then we use the diagram shown in Figure 7 (left). The costs are  $1 - \chi \leq 2(1 - \chi)$ , for  $\chi \leq 1$ . Otherwise, one of  $v, v'$  has left pivot type and the other has right pivot type, then  $p(v) = p(v')$  and  $pc(v') = v$ . As the roles of  $v$  and  $v'$  are

symmetric, we may assume w.l.o.g. that  $v$  has right pivot type and  $v'$  has left pivot type. We use the diagram shown in Figure 7 (right) for the case where  $v'$  is  $\mathcal{T}(3, \curvearrowright^2)$ ; other types are handled analogously. The costs to establish the invariants are  $1 \leq 2(1 - \chi)$ , for  $\chi \leq 1/2$ . ◀



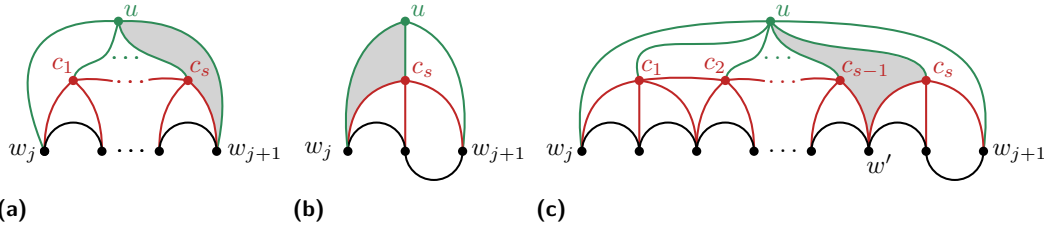
■ **Figure 7** Insertion of  $v_i$  and  $v_{i+1} = pc(v_i) \in \mathcal{E}_{i-1}$  if  $v_i$  has right pivot type.

If we can apply one of Lemmas 10 and 11, we make progress by inserting two vertices  $v_i$  and  $v_{i+1}$ . Hence, from now on, we assume that neither of Lemmas 10 and 11 can be applied. Our goal in the remainder of this section is to show that in this case we can find a vertex  $u$  that is not eligible but sufficiently close to being eligible – in a way described in the following – that we can aim to insert  $u$  next, along with some other vertices.

More specifically, the vertex  $u$  has neighbors  $w_1, \dots, w_k$  on  $P_o(G_{i-1})$ , for  $k \geq 2$ , and each subregion  $X_j$  of  $R_{i-1}(u)$  bounded by the edges  $uw_j$  and  $uw_{j+1}$  has a particularly simple structure. First of all, there exists an integer  $s = s(X_j)$  such that we have  $X_j \cap \mathcal{E}_{i-1} = \{c_1, \dots, c_s\}$ , and every  $c_\ell$ , for  $1 \leq \ell \leq s$ , is adjacent to  $u$  in  $G$ . We distinguish three types of regions, depending on whether  $X_j$  contains eligible vertices of left, right, or both pivot types.

**Left-pivot region.** (see Figure 8a)

- Every  $c_\ell$ , for  $1 \leq \ell \leq s$ , has left pivot type.
- We have  $pc(c_1) = u$  and  $pc(c_\ell) = c_{\ell-1}$ , for all  $2 \leq \ell \leq s$ .
- All vertices in  $(V \setminus \mathcal{E}_{i-1}) \cap X_j$  lie inside the face bounded by  $uc_s w_{j+1}$ .



■ **Figure 8** Structure of regions that our to-be-inserted-next vertex  $u$  spans with  $P_o(G_{i-1})$ . All eligible vertices (shown red) are adjacent to  $u$ , all other vertices lie inside the shaded region.

**Right-pivot region.** (see Figure 8b)

- We have  $s = 1$ , the vertex  $c_1$  has right pivot type, and  $pc(c_1) = u$ .
- All vertices in  $(V \setminus \mathcal{E}_{i-1}) \cap X_j$  lie inside the face bounded by  $uw_j c_1$ .

**Both-pivot region.** (see Figure 8c)

- Every  $c_\ell$ , for  $1 \leq \ell \leq s - 1$ , has left pivot type and  $c_s$  has right pivot type.
- We have  $pc(c_1) = pc(c_s) = u$  and  $pc(c_\ell) = c_{\ell-1}$ , for all  $2 \leq \ell \leq s - 1$ .
- The rightmost neighbor of  $c_{s-1}$  on  $P_o(G_{i-1})$  is the same as the leftmost neighbor of  $c_s$  on  $P_o(G_{i-1})$ ; denote this vertex by  $w'$ .
- All vertices in  $(V \setminus \mathcal{E}_{i-1}) \cap X_j$  lie inside the quadrilateral  $uc_{s-1}w'c_s$ .



**How to select  $u$ .** In the remainder of this section we will sketch how to select a suitable vertex  $u$  such that all regions spanned by  $u$  and  $P_o(G_{i-1})$  have the nice structure explained above. The first part of the story is easy to tell: We select  $u$  to be a minimal (w.r.t.  $\prec$ ) element of the set  $\mathcal{U} := \{\text{pc}(v) : v \in \mathcal{E}_{i-1}\} \setminus \mathcal{E}_{i-1}$ . Such a vertex always exists because

► **Lemma 12.** *We have  $\mathcal{U} \neq \emptyset$ .*

As there is a vertex  $v \in \mathcal{E}_{i-1}$  with  $u = \text{pc}(v)$ , we know that  $u \in \mathcal{U}$  has at least one neighbor on  $P_o(G_{i-1})$ , which is  $\text{p}(v)$ . By Lemma 10 we may assume  $d_{i-1}(u) \geq 2$ . Let  $w_1, \dots, w_k$  denote the sequence of neighbors of  $u$  along  $P_o(G_{i-1})$ . The edges  $uw_j$ , for  $2 \leq j \leq k-1$ , split  $R_{i-1}(u)$  into  $k-1$  subregions; let  $X_j$  denote the (open) region bounded by  $w_juw_{j+1}$  and the part of  $P_o(G_{i-1})$  between  $w_j$  and  $w_{j+1}$ , for  $1 \leq j < k$ .

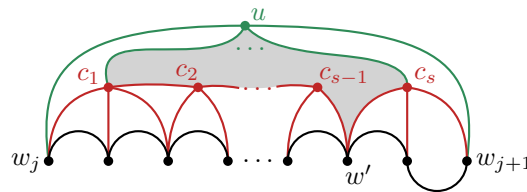
► **Lemma 13.** *In every region  $X_j$ , for  $1 \leq j < k$ , there is at most one eligible vertex  $v$  of each pivot type for which  $\text{pc}(v) = u$ .*

► **Lemma 14.** *In every region  $X_j$ , at most one eligible vertex has right pivot type. If there exists a vertex  $v \in X_j \cap \mathcal{E}_{i-1}$  that has right pivot type, then  $\text{pc}(v) = u$ .*

► **Lemma 15.** *Let  $Q$  denote the set of vertices in  $X_j \cap \mathcal{E}_{i-1}$  that have left pivot type. If  $Q \neq \emptyset$ , then the vertices in  $Q$  form a sequence  $x_1, \dots, x_q$ , for some  $q \geq 0$ , such that  $x_j = \text{pc}(x_{j+1})$ , for  $1 \leq j \leq q-1$ , and  $\text{pc}(x_1) = u$ .*

► **Lemma 16.** *Let  $e \in P_o(G_{i-1}) \cap \partial X_j$ , for some  $1 \leq j < k$ , and let  $c_e \in V \setminus V_{i-1}$  denote the vertex that covers  $e$ . Then either  $c_e = u$  or  $c_e \in \mathcal{E}_{i-1}$ .*

We process the regions  $X_1, \dots, X_{k-1}$  together with  $u$ . Consider region  $X_j$  such that  $X_j \cap V \neq \emptyset$ , and denote  $E_j = P_o(G_{i-1}) \cap \partial X_j$ . By Lemma 16 the vertices that cover one or more edges of  $E_j$  are exactly the vertices in  $\mathcal{E}_{i-1} \cap X_j$ . Thus, we can order these vertices from left to right, according to the edge(s) in  $E_j$  they cover. Denote this sequence by  $c_1, \dots, c_s$ . By Lemma 14 the only vertex in  $X_j \cap V$  that may have right pivot type is  $c_s$ . Denote  $s' = s-1$  if  $c_s$  has right pivot type, and  $s' = s$ , otherwise; i.e.,  $c_{s'}$  is the rightmost vertex of the sequence that has left pivot type. By Lemma 15 we have  $c_h = \text{pc}(c_{h+1})$ , for  $1 \leq h \leq s'-1$ , and  $\text{pc}(c_1) = u$ . It follows that the rightmost vertex  $w'$  of  $P_o(G_{i-1})$  that is adjacent to  $c_{s'}$  is the only vertex of  $P_o(G_{i-1})$  that can be adjacent to a vertex in  $(X_j \cap V) \setminus \mathcal{E}_{i-1}$ . So the general situation inside  $X_j$  can be summarized as depicted in Figure 9. Neither the sequence of left pivot vertices nor the right pivot vertex may exist, but if neither is present, then  $X_j \cap V = \emptyset$ .



■ **Figure 9** The structure of eligible vertices within a region  $X_j$ . All triangular faces here are empty, only the central face (shaded) may contain other vertices or edges  $uc_h$ , for  $2 \leq h < s$ . The left pivot vertices could be of any type  $\mathcal{T}(z, \prec^{z-1})$ .

The following lemma allows us to assume that the central face in each region  $X_j$  is subdivided into empty (of vertices) triangles and at most one – not necessarily empty – triangle or quadrilateral (the latter if  $X_j$  contains eligible vertices of both pivot types).

► **Lemma 17.** *Let  $X_j$  be a region s.t. there exist  $v, v' \in \mathcal{E}_{i-1} \cap X_j$  with  $\text{pc}(v) = v'$ , let  $v''$  be the vertex that covers  $vv'$ . If  $v'' \neq u$  and  $\chi \leq 1/5$ , there exist  $v_i, \dots, v_{i+h-1}$  with  $h \geq 3$  s.t. a valid diagram for  $G_{i+h-1}$  can be obtained by spending at most  $(1 - \chi)h$  credits.*

**Proof.** By Lemma 14 both  $v$  and  $v'$  have left pivot type. In particular, if  $c_s \neq c_{s'}$ , this implies that we have  $v, v' \neq c_s$  (see also Figure 9). By planarity and as  $v'' \neq u$ , we have  $v'' \in X_j$ . If  $v''$  is not adjacent to  $w'$ , then  $v''$  is eligible after adding  $v$  and  $v'$  and we can set  $v_i = v$ ,  $v_{i+1} = v'$ , and  $v_{i+2} = v''$  and use the diagram for  $G_{i+2}$  shown in Figure 10 (left), for a cost of  $2 + 2\chi \leq 3 - 3\chi$ , for  $\chi \leq 1/5$ . The figure shows the drawing where both  $v$  and  $v'$  are  $\mathcal{T}(2, \frown)$ ; it easily extends to the types  $\mathcal{T}(3, \frown^2)$  and  $\mathcal{T}(4, \frown^3)$  because more mountains to the right of  $v$  can be paid for by the corresponding mountains whose left endpoint is covered by  $v$  and for more mountains to the left of  $v'$  their left endpoint is covered by  $v'$ .

Otherwise,  $v''$  is adjacent to  $w'$ . We claim that we may assume  $v = c_{s'}$  and  $v' = c_{s'-1}$ . To see this let  $\tilde{v} \neq v''$  be the vertex that covers  $c_{s'-1}c_{s'}$  and observe that  $\tilde{v}$  is enclosed by a cycle formed by  $vv''w'$  and the part of  $P_o(G_{i-1})$  between the right neighbor of  $v$  and  $w'$ . In particular, we have  $\tilde{v} \neq u$  and so  $c_{s'-1}, c_{s'}, \tilde{v}$  satisfy the conditions of the lemma, as claimed. We set  $v_i = v$  and  $v_{i+1} = v'$ , and use the diagram shown in Figure 10 (right). If  $v''$  is eligible in  $G_{i+1}$ , that is, the triangle  $vv''w'$  is empty of vertices, then we set  $v_{i+2} = v''$  and have a diagram for  $G_{i+2}$  for a cost of  $2 + \chi \leq 3 - 3\chi$ , for  $\chi \leq 1/4$ .

Otherwise, by Lemma 7 we inductively obtain a valid diagram  $D$  for the subgraph of  $G$  induced by taking  $vv''w'$  as an outer triangle together with all vertices inside, with  $v''v$  as a starting edge and  $w'$  as a last vertex. Then we plug  $D$  into the triangle  $vv''w'$  as shown in Figure 10 (right). All mountains of  $D$  with left endpoint  $v''$  carry a credit by (X2) for  $D$ . Thus, the resulting diagram is extensible. For the costs we have to account for the fact that  $w'$  is considered to contribute  $1 - \chi$  credits to  $D$ , whereas we had already accounted for  $w'$  in the diagram for  $G_{i-1}$ . On the other hand, the edge  $v''w'$  is paid for as a part of  $D$ . Thus, the additional costs to handle  $v, v', v''$  are  $(1 - \chi) + 1 + \chi = 2 \leq 3 - 3\chi$ , for  $\chi \leq 1/3$ . ◀



■ **Figure 10** Two vertices  $v, v'$  that have left pivot type and  $v'' \neq u$  covers the edge  $vv'$ .

To complete the proof of Lemmas 6 and 7 it remains to insert  $u$  along with the set  $\mathcal{V}_u := V \cap R_{i-1}(u)$  of all vertices inside  $X_1, \dots, X_{k-1}$ , at a cost of  $1 - \chi$  credits per vertex. We process these regions from right to left in two phases: In Phase 1, we select a suitable collection  $X_j, \dots, X_{k-1}$  of regions, for some  $j \in \{1, \dots, k - 1\}$ , so that we can insert  $u$  together with all the vertices inside these regions. Then in Phase 2, we process the remaining regions, assuming that  $u$  is already placed on the spine, somewhere to the right. To achieve this we do a case analysis, depending on the four types of regions: left, right, both pivot, or empty. In Appendix E of the full version, we show that in all cases  $u \cup \mathcal{V}_u$  can be inserted as required.

## 5 Triangulations with many degree three vertices

► **Theorem 18.** *Let  $G$  be a triangulation with  $n$  vertices, and let  $d$  denote the number of degree three vertices in  $G$ . Then  $G$  admits a monotone plane arc diagram with at most  $n - d - 4$  biarcs, where every biarc is down-up.*

**Proof Sketch.** Let  $T$  denote the triangulation that results from removing all degree-3 vertices from  $G$ , i.e.,  $T$  has  $k = n - d$  vertices. We proceed in two steps; see Appendix F of the full version for details.



■ **Figure 11** Insert a vertex using at most one credit and make every triangle cross the spine.

**First step.** We draw  $T$  while maintaining Invariants (X1)–(X3) and (X5) using the following modifications of our default insertion rules; see Figure 11. First, if we insert  $v_i$  into a pocket, we always ensure that the leftmost edge incident to  $v_i$  is a mountain. Second, if all edges covered by  $v_i$  are mountains, we *push down* the leftmost such mountain  $m$ , that is, we redraw  $m$  and all mountains having the same left endpoint as  $m$  into down-up biarcs. Third, instead of assigning credits to covered mountains whose left endpoint remains on the outer face, we immediately transform them into biarcs. Fourth, each vertex aside from  $v_1, v_2, v_3, v_n$  contributes 1 credit to the charging scheme. As a result, the arc diagram of  $T$  has at most  $n - d - 4$  biarcs and all created faces have a non-empty intersection with the spine – note that the latter property does not follow from the result by Cardinal et al. [2, 3].

**Second step.** We insert each degree-three vertex  $v$  in its containing face  $f$  of  $T$ . Using that  $f$  crosses the spine we can place  $v$  there and then realize each edge to a vertex of  $f$  as a proper arcs. Thus, no new biarcs are created in the second step. ◀

▶ **Theorem 2.** *Every Kleetope on  $n$  vertices admits a monotone plane arc diagram with at most  $\lfloor (n - 8)/3 \rfloor$  biarcs, where every biarc is down-up.*

**Proof.** Let  $G$  be a Kleetope on  $n$  vertices, and let  $d$  denote the number of degree three vertices in  $G$ . By Theorem 18 the graph  $G$  admits a monotone plane arc diagram with at most  $n - d - 4$  biarcs, where every biarc is down-up. Removing the degree three vertices from  $G$  we obtain a triangulation  $T$  on  $n - d$  vertices, which by Euler's formula has  $2(n - d) - 4$  triangular faces. As  $G$  is a Kleetope, it is obtained by inserting a vertex into each of these faces, that is, we have  $n = (n - d) + 2(n - d) - 4$  and thus  $d = (2n - 4)/3$ . So there are at most  $n - d - 4 = (n - 8)/3$  biarcs in the diagram. ◀

## 6 Planar 3-Trees

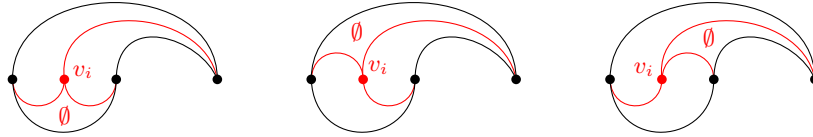
For 3-trees it is natural to follow their recursive construction sequence and build a corresponding diagram incrementally. A planar 3-tree  $G$  is built by starting from a (combinatorial) triangle. At each step we insert a new vertex  $v$  into a (triangular) face  $f$  of the graph built so far, and connect  $v$  to the three vertices of  $f$ . Every planar 3-tree  $G$  on at least four vertices is 3-connected. So its combinatorial embedding is unique, and for each triangle of the abstract graph we know whether it is facial or separating. In the former case, there is exactly one vertex of  $G$  that is adjacent to all vertices of the triangle, in the latter case there are exactly two such vertices. In particular, we can pick any facial triangle to be the starting triangle of our construction sequence for  $G$  and become the outer face of our diagram.

## 11:12 Monotone Arc Diagrams with Few Biarcs

Let  $v_1, \dots, v_n$  be such a construction sequence for  $G$ . For  $i \in \{3, \dots, n\}$ , let  $V_i = \{v_1, \dots, v_i\}$  and  $G_i = G[V_i]$ . Each vertex  $v_i$ , for  $i \in \{4, \dots, n\}$ , is inserted into a face  $F(v_i) = uvw$  of  $G_{i-1}$ , creating three *child faces*  $uvv_i$ ,  $vvv_i$  and  $wvv_i$  of  $uvw$  in  $G_i$ . We also say that  $v_i$  is the *face vertex*  $v(uvw)$  of face  $uvw$ . We call a face  $f$  of  $G_i$  *active* if it has a face vertex in  $V \setminus V_i$ ; otherwise, it is *inactive*. The *grand-degree*  $\text{gd}(f)$  is the maximum number of active child faces of  $f$  in all of  $G_3, \dots, G_n$ . Observe that by construction  $\text{gd}(f) \in \{0, \dots, 3\}$  and that  $f$  is active for some  $G_i$  if and only if  $\text{gd}(f) > 0$ . Similarly, a vertex is a *gd- $i$*  vertex, for  $i \in \{0, 1, 2, 3\}$ , if it is the face vertex of a face  $f$  with  $\text{gd}(f) = i$ . For a construction sequence we define its dual *face tree*  $\mathcal{T}$  on the faces of all  $G_i$  such that the root of  $\mathcal{T}$  is  $v_1v_2v_3$ , and each active face  $uvw$  has three children: the faces  $uvz$ ,  $vwz$ , and  $wuz$ , where  $z = v(uvw)$ . Note that the leaves of  $\mathcal{T}$  are inactive for all  $G_i$ . Let us first observe that no biarcs are needed if all faces have small grand-degree. To this end, also recall that  $G$  admits a plane proper arc diagram if and only if it is subhamiltonian and planar.

► **Theorem 19.** *Let  $G$  be a planar 3-tree that has a construction sequence  $v_1, \dots, v_n$  such that for each face  $f$  in its dual tree  $\text{gd}(f) \leq 2$ . Then  $G$  admits a plane proper arc diagram.*

**Proof.** We start by drawing the face  $v_1v_2v_3$  as a *drop*, that is, a face where the two short edges are proper arcs on different sides of the spine; see Figure 12. Then we iteratively insert the vertices  $v_i$ , for  $i = 4, \dots, n$ , such that every face that corresponds to an internal vertex of the dual tree  $\mathcal{T}$  is a drop in the diagram  $D_i$  for  $G_i$ . This can be achieved because by assumption at least one of the three faces of  $D_i$  created by inserting  $v_i$  is a leaf of  $\mathcal{T}$ , which need not be realized as a drop. But we can always realize the two other faces as drops, as shown in Figure 12. In this way we obtain a diagram for  $G$  without any biarc. ◀



■ **Figure 12** Insert a vertex  $v_i$  into a drop s.t. any chosen two of the faces created are drops.

As  $\mathcal{T}$  is a tree, we can relate the number of internal vertices to the number of leaves.

► **Lemma 20.** *Let  $f_d$  denote the number of faces in  $\mathcal{T}$  with grand-degree exactly  $d$ , and let  $n_{\text{inact}}$  denote the number of face vertices that create inactive faces only. Then  $n_{\text{inact}} \geq 2f_3 + f_2$ .*

**Proof.** Consider the rooted tree  $\mathcal{T}'$  obtained by removing all leaves of  $\mathcal{T}$ , and observe that the grand-degree in  $\mathcal{T}$  corresponds to the vertex degree in  $\mathcal{T}'$ . ◀

We are now ready to describe our drawing algorithm for general planar 3-trees.

► **Theorem 3.** *Every planar 3-tree admits a plane arc diagram with at most  $\lfloor \frac{3}{4}(n-3) \rfloor$  biarcs that are all down-up monotone.*

**Proof.** Our algorithm is iterative and draws  $G$  in the sequence prescribed by  $\mathcal{T}$ . Namely, at each step of our algorithm, we select an arbitrary already drawn face  $uvw$  and insert its face vertex  $v(uvw)$ , possibly together with the face vertex of a child face. We will consider faces of a particular shape mostly. Consider a face  $f = uvw$  such that  $u, v, w$  appear in this order along the spine and  $uw$  forms the upper envelope of  $f$ . (There is a symmetric configuration, obtained by a rotation by an angle of  $\pi$  where  $uw$  forms the lower envelope of  $f$ .) We say

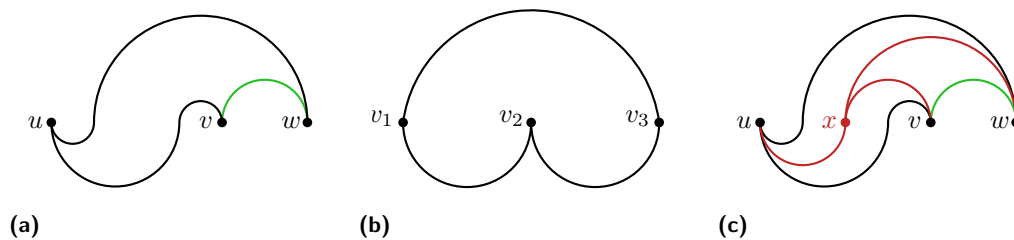
that  $f$  is *ottifant-shaped*<sup>4</sup> if it contains a region bounded by a down-up biarc between  $u$  and  $w$ , a down-up biarc between  $u$  and  $v$  and a mountain between  $v$  and  $w$ ; see Figure 13a. Note the word “contains” in the definition of ottifant-shaped, which allows the actual face to be larger. For instance, the top boundary could be a mountain, but we treat it as if it was a biarc for the purposes of drawing edges; that is, we only connect to  $u$  from below the spine.

To control the number of biarcs drawn we maintain a charge  $\text{ch}(v)$  for each vertex  $v$ . We require additional flexibility from the edge  $vw$  of an ottifant-shaped face  $f = uvw$ , which we call the *belly* of  $f$ . To this end, we call a mountain  $vw$  *transformable* if it can be redrawn as a down-up biarc for at most  $3/2$  units of charge. (Note that every edge can be drawn as a biarc for only one credit. But in some cases redrawing an edge as a biarc requires another adjacent edge to be redrawn as a biarc as well. Having an extra reserve of half a credit turns out sufficient to cover these additional costs, as shown in the analysis below.)

More specifically, we maintain the following invariants:

- (O1) Each internal active face is ottifant-shaped.
- (O2) If the belly of an active face is a mountain, it is transformable.
- (O3) The sum of the charges of all vertices is at least the number of biarcs drawn.
- (O4) For each vertex  $v$  we have  $\text{ch}(v) \leq \frac{3}{4}$ .

It is easy to see that a drawing  $D$  of  $G$  has at most  $\lfloor \frac{3}{4}n \rfloor$  biarcs if the invariants hold for  $D$ .



■ **Figure 13** (a) An ottifant-shaped face  $uvw$ , where the long edge is on the top page (green edges are transformable). (b) Drawing of the initial face  $v_1v_2v_3$ . (c) Insertion of a gd-1 vertex  $x = v(uvw)$ .

**Initialization.** We put  $v_1v_2v_3$  on the spine in this order and draw the edges  $v_1v_2$  and  $v_2v_3$  as pockets and  $v_1v_3$  as a mountain; see Figure 13b. The invariants (O1)–(O4) hold.

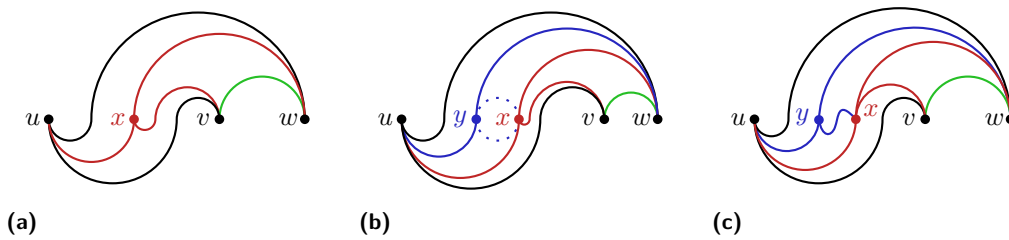
**Charging rights.** Typically we charge a vertex when it is added to the drawing. But different vertices have different needs. Specifically, we will see that no biarc/charge is used when inserting a gd-0 vertex. Therefore, for each gd-0 vertex  $v$  we distribute the rights to use the charge of  $v$  among two targets: (1) the *parent* of  $v$  (i.e., the vertex  $v(f)$  of the parent  $f$  of  $F(v)$  in  $\mathcal{T}$ ) – if it exists – may assign a charge of  $\leq 1/4$  to  $v$  and (2) the so-called *preferred ancestor*  $p(v)$  may assign a charge of  $\leq 1/2$  to  $v$ . Preferred ancestors are determined by selecting an arbitrary surjective map  $p$  from the set of gd-0 vertices to the set of gd-2 and gd-3 vertices. According to Lemma 20 there exists such a map such that every gd-2 is selected at least once and every gd-3 vertex is selected at least twice as a preferred ancestor.

<sup>4</sup> An *ottifant* is a cartoon abstraction of an elephant designed and popularized by the artist Otto Waalkes. Use of the term *ottifant* with kind permission of Ottifant Productions GmbH.

**Iterative step.** We select an arbitrary active face  $f = uvw$ , which is ottifant-shaped by (O1), and insert its face vertex  $x := v(f)$  into  $f$ . Assume w.l.o.g. (up to rotation by an angle of  $\pi$ ) that  $uw$  forms the top boundary of  $f$ . We make a case distinction based on  $\text{gd}(f)$ .

**Case 1:**  $\text{gd}(f) = 0$ . Then all child faces of  $f$  are inactive so that (O1) and (O2) hold trivially. We insert  $x$  inside  $f$  between  $u$  and  $v$  on the spine, draw the edge  $ux$  as a pocket and  $xv$  and  $xw$  as mountains; see Figure 13c. No biarcs are created, so (O3)–(O4) hold.

**Case 2:**  $\text{gd}(f) \geq 2$ . We insert  $x$  as in Case 1, except that  $xv$  is drawn as a biarc rather than as a mountain; see Figure 14a. All created child faces are ottifant-shaped (O1) and all bellies are transformable (O2). We created one biarc. So to establish (O3)–(O4) it suffices to set  $\text{ch}(x) = \frac{3}{4}$  and add a charge of  $\frac{1}{4}$  to one of the (at least one)  $\text{gd}-0$  vertices in  $p^{-1}(x)$ .



■ **Figure 14** Insertion of (a) a  $\text{gd}-2$  vertex  $x$ ; (b) a  $\text{gd}-1$  vertex  $y$ ; (c) a  $\text{gd}-2$  vertex  $y$ .

**Case 3:**  $\text{gd}(f) = 1$ . Then only one of the three child faces of  $f$  is active. If  $uvx$  is the active child face, then we use the same drawing as for a  $\text{gd}-0$  vertex (see Figure 13c) and all invariants hold. However, if one of the other child faces is active, then we cannot use this drawing because  $xw$  is not transformable and  $xvw$  is not ottifant-shaped.

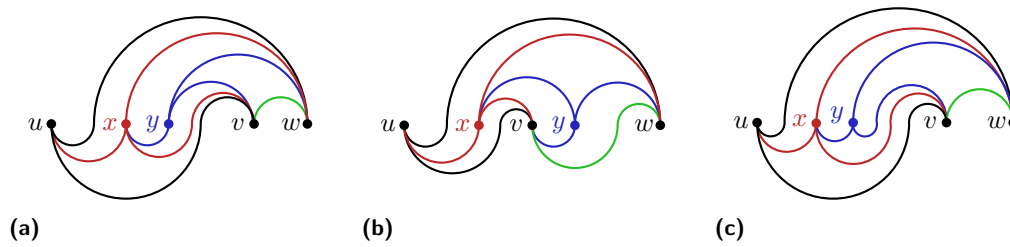
So we also consider the face vertex  $y$  of the unique child face  $f'$  of  $x$  and insert both  $x$  and  $y$  into the drawing together. We consider two subcases, according to  $f'$ .

**Case 3A:**  $f' = uxw$ . If  $\text{gd}(f') = 0$ , then we can once again use the drawing for a  $\text{gd}-0$  vertex (see Figure 13c) because  $f'$  is ottifant-shaped and none of its child faces are active.

If  $\text{gd}(f') = 1$ , then we add first  $x$  as described for a  $\text{gd}-2$  vertex above (see Figure 14a). Then we add  $y$  into  $f'$  and draw all incident edges as proper arcs; the edge  $yx$  can be drawn either as a mountain (if  $uxy$  is the active child face of  $f'$ ) or as a pocket (otherwise); see Figure 14b. In either case, invariants (O1)–(O2) hold. We added one biarc ( $xv$ ). To establish (O3)–(O4) we set  $\text{ch}(x) = \text{ch}(y) = \frac{1}{2} < \frac{3}{4}$ .

Otherwise, we have  $\text{gd}(f') \geq 2$ . We first add  $x$  as described above for a  $\text{gd}-0$  vertex and then  $y$  as a  $\text{gd}-2$  vertex; see Figure 14c. Invariant (O1) holds. To establish (O2) we have to make the bellies  $xw$  and  $uy$  of  $yxw$  and  $uyx$ , respectively, transformable. To this end, we put  $1/2$  units of charge aside so that both  $xv$  and  $xw$  could be redrawn as biarcs for  $3/2$  units of charge, as required. Moreover, we observe that  $uy$  can be transformed into a biarc for 1 units of charge if necessary as there is no other edge that must be transformed in this scenario. We also added a biarc, namely,  $yx$ . To establish (O3)–(O4) we set  $\text{ch}(x) = \text{ch}(y) = \frac{3}{4}$ .

**Case 3B:**  $f' = xv w$ . We consider several subcases according to  $\text{gd}(f')$ . If  $\text{gd}(f') = 0$ , we first insert  $x$  as described above for a  $\text{gd}-2$  vertex and then  $y$  as a  $\text{gd}-0$  vertex; see Figure 15a. Invariants (O1)–(O2) hold trivially. We used one biarc ( $xv$ ). To establish (O3)–(O4), we set  $\text{ch}(x) = \frac{3}{4}$  and increase  $\text{ch}(y)$  by  $\frac{1}{4}$ . The latter is allowed because  $x$  is the parent of  $y$ .



■ **Figure 15** Insertion of (a) a gd-2 vertex  $x$ ; (b) a gd-1 vertex  $y$ ; (c) a gd-2 vertex  $y$ .

We use the same drawing if  $\text{gd}(f') = 1$  and the (only) active child face of  $f'$  is  $xvy$  or  $xyw$ . If  $xvy$  is active, then we set  $\text{ch}(x) = \text{ch}(y) = \frac{1}{2} < \frac{3}{4}$  to establish (O3)–(O4). If  $xyw$  is active, then we put  $1/2$  units of charge aside to make  $yw$  transformable and establish (O2). Then we set  $\text{ch}(x) = \text{ch}(y) = \frac{3}{4}$  to establish (O3)–(O4).

If  $\text{gd}(f') = 1$ , then it remains to consider the case that the (only) active child face of  $f'$  is  $yvw$ . We transform  $vw$  into a biarc, then insert  $x$  between  $u$  and  $v$ , and finally insert  $y$  between  $v$  and  $w$  on the spine inside  $f$ . All edges incident to  $x$  and  $y$  are drawn as proper arcs; see Figure 15b. The only active (grand)child face of  $f$  is  $yvw$ , and (O1)–(O2) hold. We have spent  $3/2$  units of charge to transform  $vw$ , and we did not create any biarc. Thus, it suffices to set  $\text{ch}(x) = \text{ch}(y) = \frac{3}{4}$  to establish (O3)–(O4).

If  $\text{gd}(f') \geq 2$ , then we first insert  $x$  between  $u$  and  $v$  and then  $y$  between  $x$  and  $v$  on the spine inside  $f$ . Then we draw  $xv$  and  $yv$  as biarcs and the remaining edges as proper arcs such that  $xy$  is a pocket; see Figure 15c. Invariants (O1)–(O2) hold. We created two biarcs ( $xv$  and  $yv$ ). To establish (O3)–(O4), we set  $\text{ch}(x) = \text{ch}(y) = \frac{3}{4}$  and we increase the charge of a vertex in  $p^{-1}(y)$  by  $1/2$ .

It follows that (O1)–(O4) hold after each step. ◀

## 7 Conclusions

We proved the first upper bound of the form  $c \cdot n$ , with  $c < 1$ , for the number of monotone biarcs in arc diagrams of planar graphs. In our analysis, only some cases require  $\chi \leq 1/5$ , indicating a possibility to further refine the analysis to achieve an even better bound. It remains open whether there exists a “monotonicity penalty” in this problem, but we ruled out the probably most prominent class of non-Hamiltonian maximal planar graphs, the Kleetopes, as candidates to exhibit such a phenomenon. It would be very interesting to close the gap between upper and lower bounds, both in the monotone and in the general settings.

## References

- 1 Frank Bernhart and Paul C. Kainen. The book thickness of a graph. *J. Combin. Theory Ser. B*, 27:320–331, 1979. doi:10.1016/0095-8956(79)90021-2.
- 2 Jean Cardinal, Michael Hoffmann, Vincent Kusters, Csaba D. Tóth, and Manuel Wettstein. Arc diagrams, flip distances, and Hamiltonian triangulations. In *Proc. 32nd Int. Sympos. Theoret. Aspects Comput. Sci. (STACS 2015)*, volume 30 of *LIPICs*, pages 197–210, 2015. doi:10.4230/LIPICs.STACS.2015.197.
- 3 Jean Cardinal, Michael Hoffmann, Vincent Kusters, Csaba D. Tóth, and Manuel Wettstein. Arc diagrams, flip distances, and Hamiltonian triangulations. *Comput. Geom. Theory Appl.*, 68:206–225, 2018. doi:10.1016/j.comgeo.2017.06.001.
- 4 Marek Chrobak and Thomas H. Payne. A linear-time algorithm for drawing a planar graph on a grid. *Inform. Process. Lett.*, 54:241–246, 1995. doi:10.1016/0020-0190(95)00020-D.

- 5 Hubert de Fraysseix, János Pach, and Richard Pollack. Small sets supporting Fary embeddings of planar graphs. In *Proc. 20th Annu. ACM Sympos. Theory Comput. (STOC 1988)*, pages 426–433, 1988. doi:10.1145/62212.62254.
- 6 Hubert de Fraysseix, János Pach, and Richard Pollack. How to draw a planar graph on a grid. *Combinatorica*, 10(1):41–51, 1990. doi:10.1007/BF02122694.
- 7 Emilio Di Giacomo, Walter Didimo, Giuseppe Liotta, and Stephen K. Wismath. Curve-constrained drawings of planar graphs. *Comput. Geom. Theory Appl.*, 30(1):1–23, 2005. doi:10.1016/j.comgeo.2004.04.002.
- 8 Hazel Everett, Sylvain Lazard, Giuseppe Liotta, and Stephen K. Wismath. Universal sets of  $n$  points for 1-bend drawings of planar graphs with  $n$  vertices. In *Proc. 15th Int. Sympos. Graph Drawing (GD 2007)*, volume 4875 of *LNCS*, pages 345–351, 2007. doi:10.1007/978-3-540-77537-9\_34.
- 9 Hazel Everett, Sylvain Lazard, Giuseppe Liotta, and Stephen K. Wismath. Universal sets of  $n$  points for one-bend drawings of planar graphs with  $n$  vertices. *Discrete Comput. Geom.*, 43(2):272–288, 2010. doi:10.1007/s00454-009-9149-3.
- 10 Emilio Di Giacomo, Walter Didimo, Giuseppe Liotta, and Stephen K. Wismath. Drawing planar graphs on a curve. In *Proc. 13th Int. Workshop Graph-Theoret. Concepts Comput. Sci. (WG 2003)*, volume 2880 of *LNCS*, pages 192–204, 2003. doi:10.1007/978-3-540-39890-5\_17.
- 11 Francesco Giordano, Giuseppe Liotta, Tamara Mchedlidze, Antonios Symvonis, and Sue Whitesides. Computing upward topological book embeddings of upward planar digraphs. *J. Discrete Algorithms*, 30:45–69, 2015. doi:10.1016/j.jda.2014.11.006.
- 12 Michael Kaufmann and Roland Wiese. Embedding vertices at points: Few bends suffice for planar graphs. In *Proc. 6th Int. Sympos. Graph Drawing (GD 1998)*, volume 1547 of *LNCS*, pages 462–463, 1998. doi:10.1007/3-540-37623-2\_47.
- 13 Michael Kaufmann and Roland Wiese. Embedding vertices at points: Few bends suffice for planar graphs. *J. Graph Algorithms Appl.*, 6(1):115–129, 2002. doi:10.7155/jgaa.00046.
- 14 Maarten Löffler and Csaba D. Tóth. Linear-size universal point sets for one-bend drawings. In *Proc. 23rd Int. Sympos. Graph Drawing Network Visualization (GD 2015)*, volume 9411 of *LNCS*, pages 423–429, 2015. doi:10.1007/978-3-319-27261-0\_35.